

RESULTS

A. Code validation

Promvonge et al. 2014 [2] have conducted study for validating the numerical model. They experimentally examined the impact of inclined vortex rings on the thermal transfer enhancement in a spherical tube. "The study experimentally examined the impact of tilted vortex rings (VR) on thermal transfer enhancement in a steady thermal fluxed tube. The 30° tilted VRs were fitted repetitively inside the tube with different geometrical parameters of the VR, three relative ring width ratios ($BR = b/D = 0.1, 0.15$ and 0.2) and four relative ring pitch ratios ($PR = P/D = 0.5, 1.0, 1.5$ and 2.0). The experimental work was done in an open-loop experimental tool. The loop was made up of a blower, orifice meter to gauge the flow rate and the thermal transfer test tube with VR insert. The length of the copper test tube was 2000 mm, with inner diameter of 50 mm, and thickness of 1.5 mm. Comparing the existing outcomes of Nusselt number with Reynolds number with the outcomes of Promvonge et al. 2014 [1] illustrated in Figure.1."

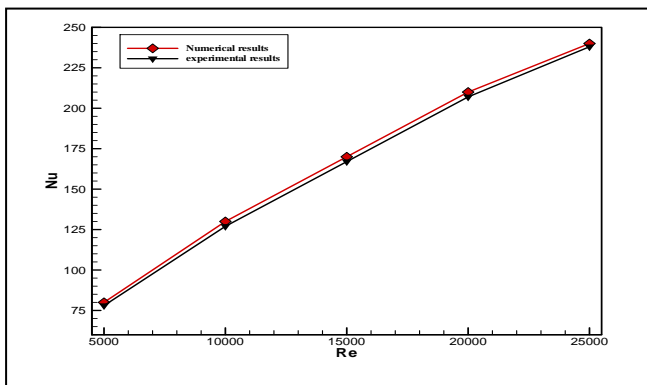


Figure 3: Comparing of the current outcomes (numerical results) with the experimental outcomes of Promvonge et al. (2014).

B. Grid independent test

case $Re=15000$, $P/D=0.5$

Based on the outcomes, it is seen that, the Nu is proportionate to the number of faces, and the Nu was 170 when number of faces was 261794. Moreover, there is no change in Nu when number of faces increasing to 282893 and 271895.

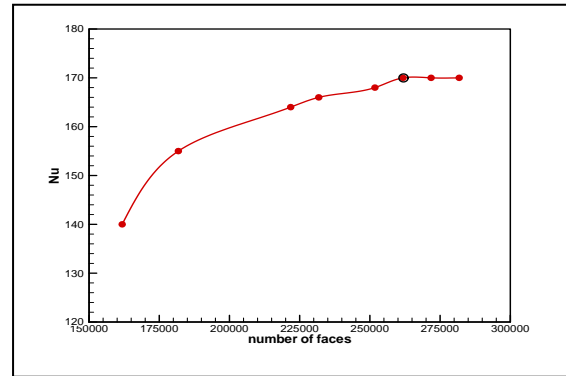


Figure 4: Grid Independence Test

C. Effect of pitch ratio $P/D=0.5$

The numerical study conducted in a tube equipped with tilted vortex rings using air as a test fluid in this case. The tilted vortex rings arrangement mounted along the test tube having slope (α) of 45° with the axial direction. Figure.2 illustrates the changes in Nusselt number while changing Reynolds number at slope of (α) of 45° for vortex rings inserts. It is noted that the Nusselt number is proportionate to Reynolds number. It also found that the Nusselt number for tubes with tilted vortex rings was greater than plain tubes. This might be attributed to the powerful turbulence intensity produced by vortex rings, which leads to quick mixing of the flow particularly at pitch ratio $P/D=0.5$.

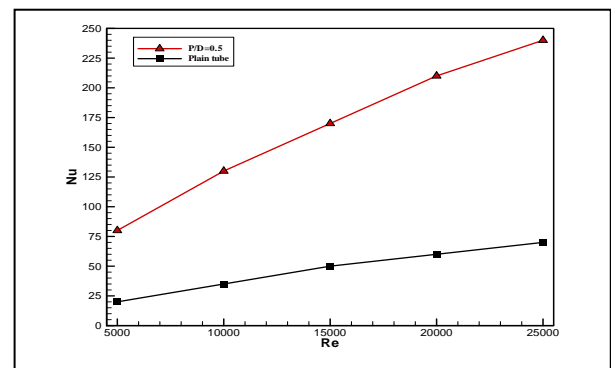


Figure 5: Variation of the Nu with Re for plain tube and tube with vortex rings inserts at pitch ratio $P/D=0.5$ and slant angle (α) of 45°

The alterations of skin friction coefficient with Reynolds number for plain tube and tube with vortex rings inserts at pitch ratio $P/D=0.5$ and slope of (α) of 45° are shown in Figure.3. It is noted that the coefficient of skin friction is disproportionate with Reynolds number. The coefficient of skin friction of the augmented tube increased little relative with the plain tube.

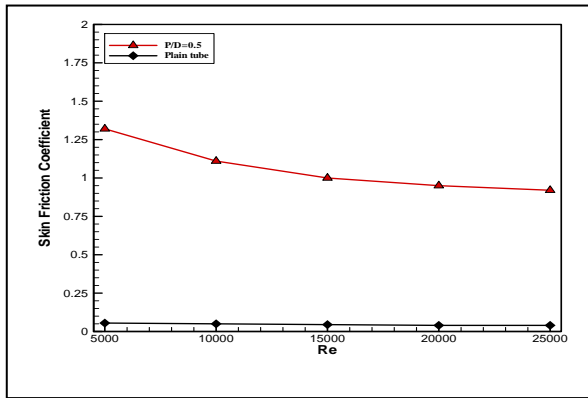


Figure 6: Variation of the skin friction coefficient with Re for plain tube and tube with vortex rings inserts at pitch ratio $P/D=0.5$ and slant angle (α) of 45°

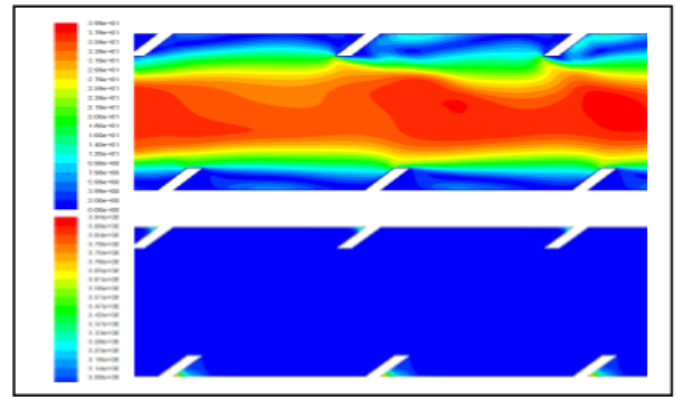


Figure 9: (Top) Velocity(m/s) and (Bottom)Temperatures (k), $P/D=0.5$, $Re=15000$

The effect of vortex rings inserts at pitch ratio $P/D=0.5$ and slant angle (α) of 45° in tube on the streamlines and isotherms at different Reynolds number 5000-25000 are presented in Figure.4, 4.5, 4.6, 4.7 and 4.8. From these figures, it is clearly found that the powerful mixing or elevated turbulence flow behind the vortex rings inserts provides many vortices which increases with increase the slant angle. The greatest mixing flow and vortices we rerecorded at slope of ($\alpha=45^\circ$).

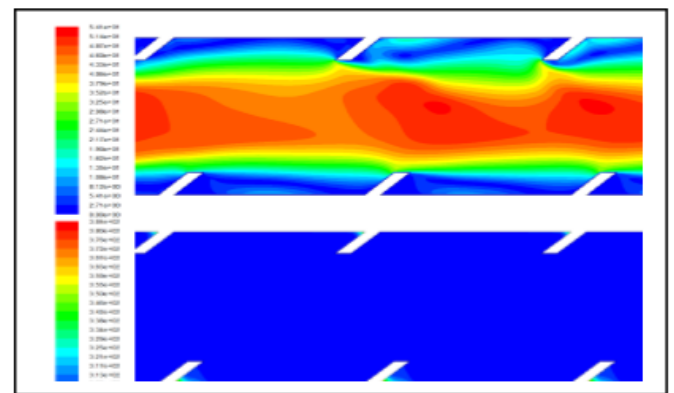


Figure 10: (Top) Velocity(m/s) and (Bottom)Temperatures (k), $P/D=0.5$, $Re=20000$

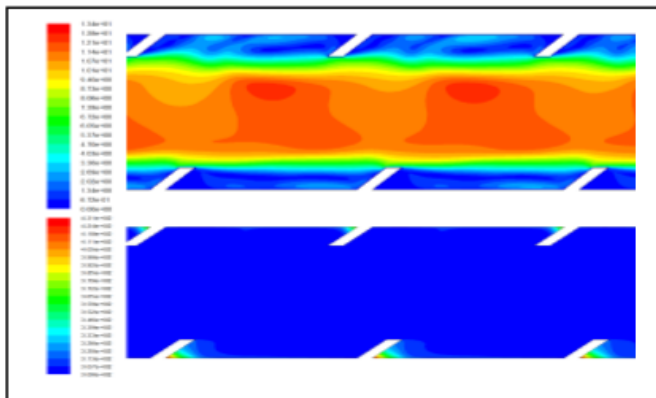


Figure 7: (Top) Velocity(m/s)and (Bottom)Temperatures(k) $P/D=0.5$, $Re=5000$

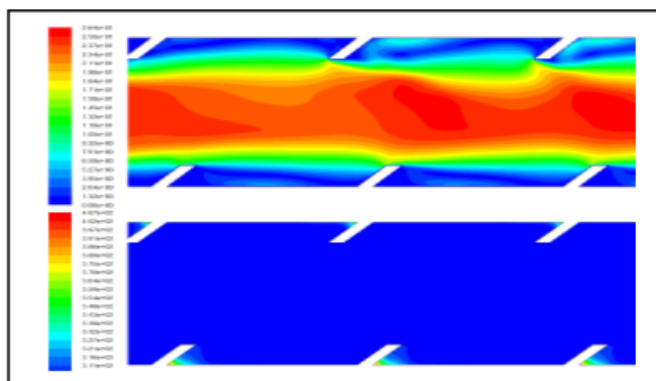


Figure 8: (Top) Velocity(m/s) and (Bottom)Temperatures (k), $P/D=0.5$, $Re=1000$

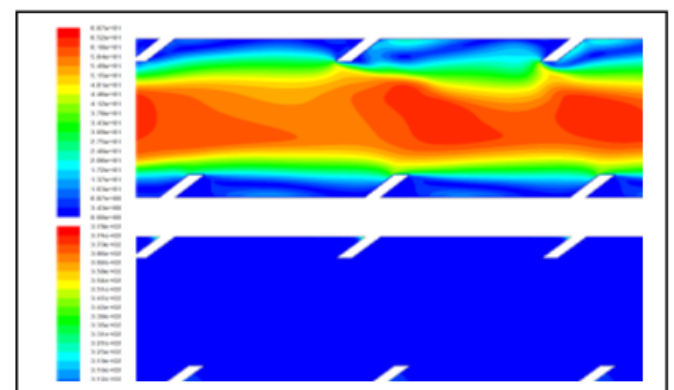


Figure 11: (Top) Velocity(m/s) and (Bottom)Temperatures (k), $P/D=0.5$, $Re=25000$

D. Effect of pitch ratio $P/D=1$

The numerical study was conducted in a tube equipped with tilted vortex rings using air as a test fluid in this experiment. The tilted vortex rings assembly was positioned along the test tube having with a slope of (α) of 45° with the axial direction. Figure.9 highlights the alteration in Nusselt number with

Reynolds number at the slope of (α) of 45° for vortex rings inserts. It can be seen that the Nusselt number is proportionate to Reynolds number. It is also found that the Nusselt number for tube with tilted vortex rings is greater than plain tube. This might be attributed to the powerful turbulence intensity produced by vortex rings, which results in quick mixing of the flow particularly at pitch ratio $P/D=1$.

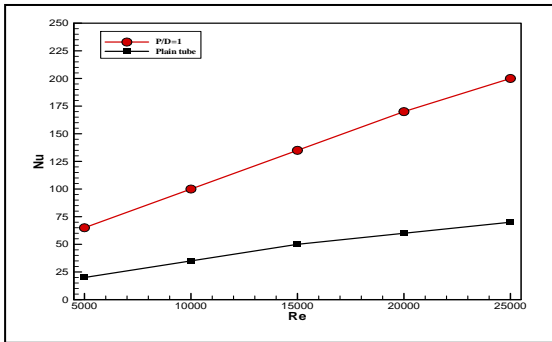


Figure 12: Variation of the Nu with Re for plain tube and tube with vortex rings inserts at pitch ratio $P/D=1$ and slant angle (α) of 45° .

The alterations in the coefficient of skin friction with Reynolds number for plain tube and tube with vortex rings inserts at pitch ratio $P/D=1$ and slant angle (α) of 45° are shown in Figure. 4.10. It is noted that the coefficient of skin friction is an inverse proportionate to Reynolds number. The coefficient of skin friction of the augmented tube increased little relative with the plain tube

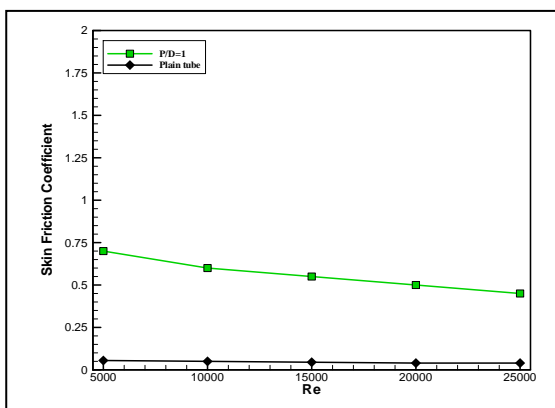


Figure 13: Variation of the skin friction coefficient with Re for plain tube and tube with vortex rings inserts at pitch ratio $P/D=1$ and slant angle (α) of 45° .

The effect of vortex rings inserts at pitch ratio $P/D=1$ and slant angle (α) of 45° in tube on the streamlines and isotherms at different Reynolds number 5000-25000 are presented in Figures 4.11, 4.12, 4.13, 4.14 and 4.15. From these figures, it is clearly found that the powerful mixing or elevated turbulence

flow behind the vortex rings inserts provide many vortices which are proportionate to the slant angle. The greatest mixing flow and vortices were recorded the slope of ($\alpha=45^\circ$).

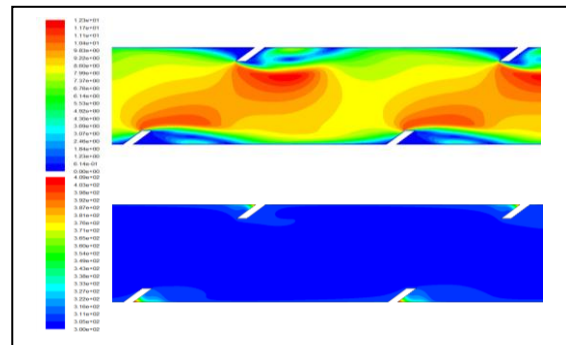


Figure 1: (Top) Velocity(m/s) and (Bottom)Temperatures (k), $P/D=1$ $Re=5000$

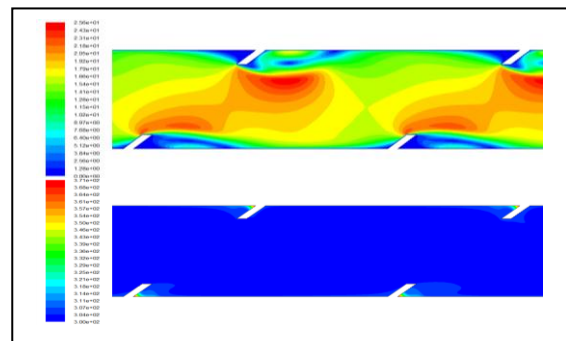


Figure 2: (Top) Velocity(m/s) and (Bottom)Temperatures (k), $P/D=1$ $Re=10000$

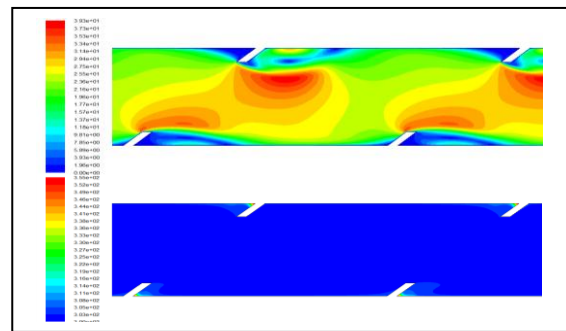


Figure 3: (Top) Velocity(m/s) and (Bottom)Temperatures (k), $P/D=1$ $Re=15000$

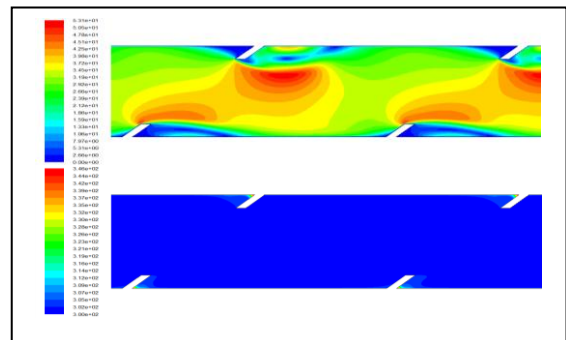


Figure 4: (Top) Velocity(m/s) and (Bottom)Temperatures (k), $P/D=1$ $Re=20000$

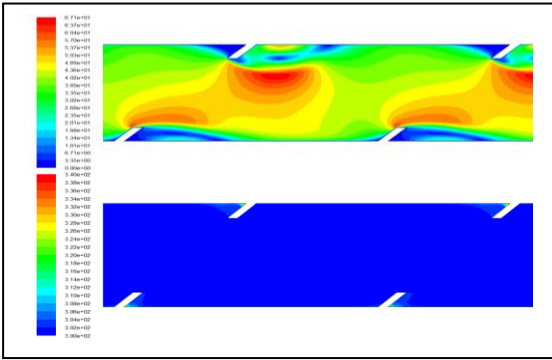


Figure 58: (Top) Velocity(m/s) and (Bottom)Temperatures (k), P/D=1 Re=25000

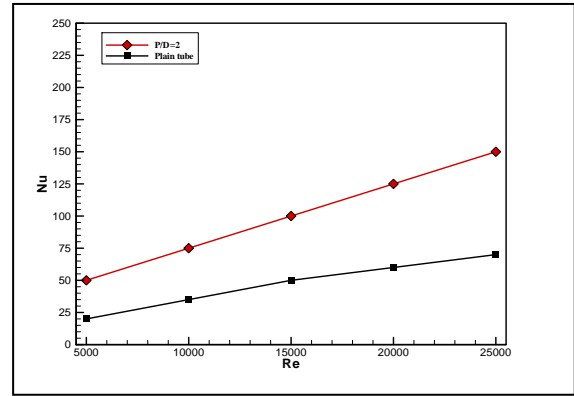


Figure 7: Variation of the skin friction coefficient with Re for plain tube and tube with vortex rings inserts at pitch ratio P/D=2 and slant angle (α) of 45° .

E. Impact of pitch ratio P/D=2

The numerical study was conducted in a tube supplemented with tilted vortex rings using air as a test fluid in this experiment. The tilted vortex rings arrangement was fixed along the test tube having slope of (α) of 45° with the axial direction. Figure.16 illustrates the alterations in Nusselt number with Reynolds number at slope of (α) of 45° for vortex rings inserts. It is found that the Nusselt number is proportionate to Reynolds number. It also found that the Nusselt number for tube with tilted vortex rings was greater than that of the plain tube. This might be attributed to a powerful turbulence intensity produced by vortex rings which leads to quick mixing of the flow particularly at pitch ratio P/D=2.

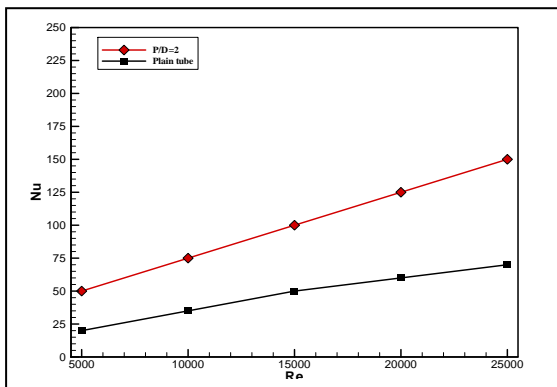


Figure 6: Variation of the Nu with Re for plain tube and tube with vortex rings inserts at pitch ratio P/D=2 and slant angle (α) of 45° .

The alterations in the coefficient of skin friction with Reynolds number for plain tube and tube with vortex rings inserts at pitch ratio P/D=2 and slant angle (α) of 45° are shown in Figure.17. It is noted that the coefficient of skin friction is inversely proportionate to Reynolds number. The coefficient of skin friction of the augmented tube increased little relative with the plain tube.

The effect of vortex rings inserts at pitch ratio P/D=2 and slant angle (α) of 45° in tube on the streamlines and isotherms at different Reynolds number 5000-25000 are presented in Figure.18, 4.19, 4.20, 4.21 and 4.22. From these figures, it is clearly found that the powerful mixing or great turbulence flow behind the vortex rings inserts provides many vortices which are proportionate to the slant angle. The greatest mixing flow and vortices was recorded at the slope of ($\alpha=45^\circ$).

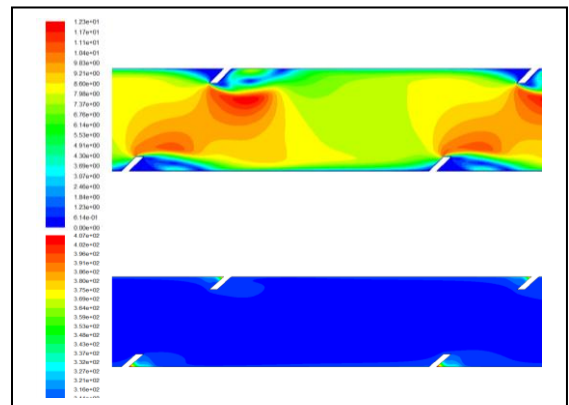


Figure 21: (Top) Velocity(m/s) and (Bottom)Temperatures (k), P/D=2 Re=5000

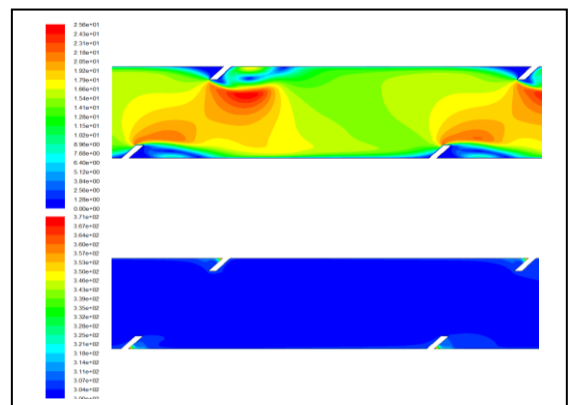


Figure 22: (Top) Velocity(m/s) and (Bottom)Temperatures (k), P/D=2 Re=10000

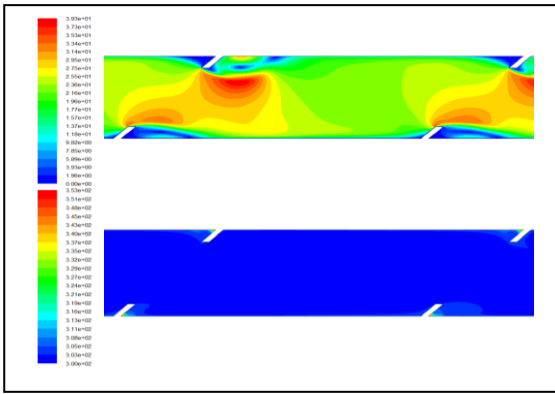


Figure 23: (Top) Velocity(m/s) and (Bottom)Temperatures (k) , P/D=2 Re=15000

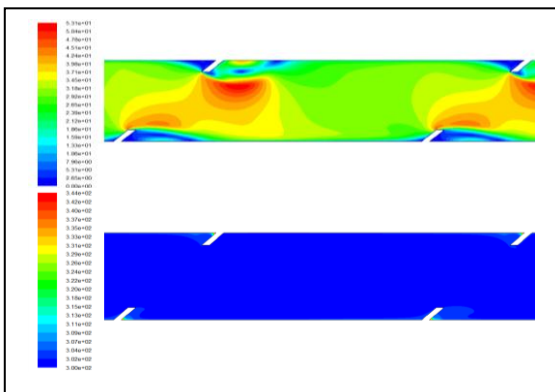


Figure 24: (Top) Velocity(m/s) and (Bottom)Temperatures (k), P/D=2 Re=20000

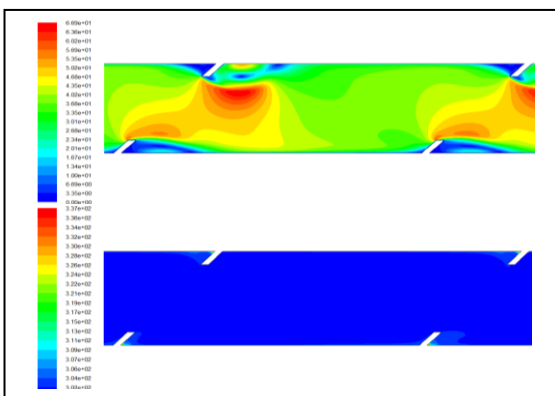


Figure 8: (Top) Velocity(m/s) and (Bottom)Temperatures (k), P/D=2 Re=25000

Figure.23 depicts all the data in order to compare the effect of vortex rings inserts at different pitch ratio P/D=0.5,1 and 2 and slant angle (α) of 45° on Nusselt number at different Reynolds number. From this figure it is found that the maximum Nusselt number can be achieved by using a lower pitch ratio P/D alongside a relatively minor pitch (P=25mm).The use of the vortex rings inserts in tube offers (i) powerful mixing or turbulence flow ahead of the vortex rings which result in destructing the thermal boundary layer and (ii)

the powerful vortices of flow which creates more effective flow mixing between the fluid at the core and the tube wall. These two flow phenomena boost an rise in the intensity of turbulence.

DISCUSSION

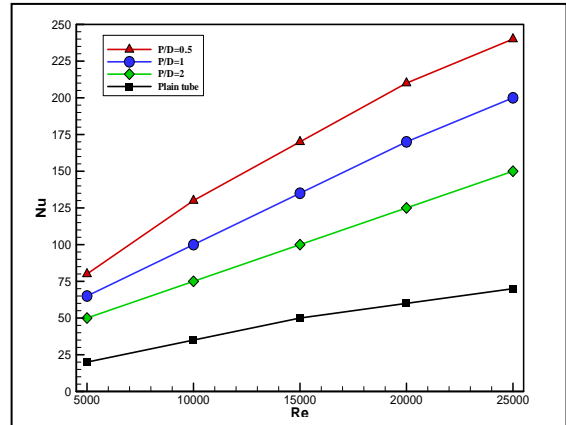


Figure 9: Variation of the Nu with Re for plain tube and tube with vortex rings inserts at different pitch ratio P/D=0.5,1 and 2 and slant angle (α) of 45° .

The result of simulation are presented in terms of Nusselt number, skin friction coefficient plots with different parameters, streamlines and iso therms. All the present results are based on the turbulent convection flow in tube with vortex rings inserts at different pitch ratio P/D=0.5,1 and 2 and slant angle (α) of 45° .The effect of vortex rings inserts on Nu, skin friction coefficient were investigated Numerically by using CFD software. The results can be fully utilized in many engineering applications in order to design heat exchanger with maximum heat transfer enhancement and reduce the cost and size of heat exchanger.

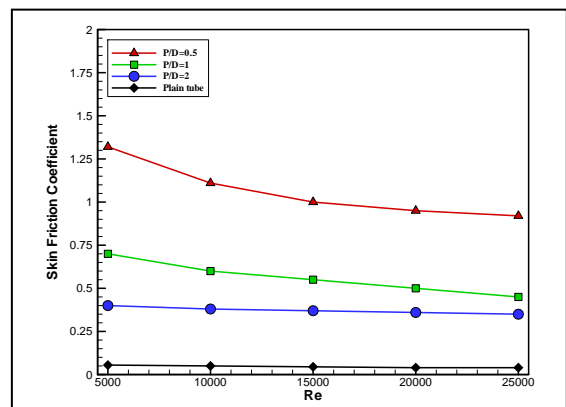


Figure 10: Variation of the skin friction coefficient with Re plain tube and tube with vortex rings inserts at different pitch ratio P/D=0.5, 1 and 2 and slant angle (α) of 45° .

CONCLUSION

An inclined vortex rings inserts were utilized to enhance the convective thermal transfer of turbulent flow in a circular tube with steady thermal flux on the top and bottom walls. The Nusselt number and the coefficient of skin friction obtained by a numerical simulation. These are the conclusions drawn:

1. The Nusselt number augmented by around 4 times for the inclined vortex rings inserts than that of the plain tube, which confirms that the inclined vortex rings inserts have a good impact upon the heat transfer augmentation.
2. The coefficient of skin friction is inversely proportionate to Reynolds number.
3. The coefficient of skin friction of the augmented tube increased little relative with the plain tube.
4. The maximum Nusselt number can be achieved by using a lower pitch ratio $P/D=0.5$ together with a relatively small pitch ($P=25\text{mm}$).
5. The maximal coefficient of skin friction for all cases is found when the pitches ratio $P/D=0.5$ and pitch is $P=25\text{mm}$.
6. The Nusselt number is considerably proportionate to Reynolds number, Re in the range of 5000-25000

REFERENCES

- [1] San, J. Y., Huang, W. C., & Chen, C. A. (2015). Experimental investigation on heat transfer and fluid friction correlations for circular tubes with coiled-wire inserts. *International Communications in Heat and Mass Transfer*, 65, 8-14.
- [2] Teerapat Chompookham, Chinaruk Thianpong, Sutapat Kwankaomeng, Pongjet Promvonge. (2010) "Heat transfer augmentation in a wedge-ribbed channel using winglet vortex generators". *International Communications in Heat and Mass Transfer*. p163-169.
- [3] García, A., Martín, R. H., & Pérez-García, J. (2013). Experimental study of heat transfer enhancement in a flat-plate solar water collector with wire-coil inserts. *Applied Thermal Engineering*, 61(2), 461-468.
- [4] Kumar, A., Kumar, M., & Chamoli, S. (2016). Comparative study for thermal-hydraulic performance of circular tube with inserts. *Alexandria Engineering Journal*
- [5] Deshmukh, P. W., & Vedula, R. P. (2014). Heat transfer and friction factor characteristics of turbulent flow through a circular tube fitted with vortex generator inserts. *International Journal of Heat and Mass Transfer*, 79, 551-560.
- [6] Eiamsa-Ard, S., & Promvonge, P. (2011). Influence of double-sided delta-wing tape insert with alternate-axes on flow and heat transfer characteristics in a heat exchanger tube. *Chinese Journal of Chemical Engineering*, 19(3), 410-423.
- [7] Prasad, P. D., Gupta, A. V. S. S. K. S., Sreeramulu, M., Sundar, L. S., Singh, M. K., & Sousa, A. C. (2015). Experimental study of heat transfer and friction factor of Al₂O₃ nanofluid in U-tube heat exchanger with helical tape inserts. *Experimental Thermal and Fluid Science*, 62, 141-150.
- [8] Noothong, W., Suwannapan, S., Thianpong, C., & Promvonge, P. (2015). Enhanced heat transfer in a heat exchanger square-duct with discrete V-finned tape inserts. *Chinese Journal of Chemical Engineering*, 23(3), 490-498.
- [9] Reay, D. A. (1991). Heat transfer enhancement-a review of techniques and their possible impact on energy efficiency in the cover Systems and CHP, 11(1), 1- 40.
- [10] Azari, & Derakhshandeh, M. (2015). An experimental comparison of convective heat transfer and friction factor of Al₂O₃ nanofluids in a tube with and without butterfly tube inserts. *Journal of the Taiwan Institute of Chemical Engineers*, 52, 31-39.